Hindawi Publishing Corporation
Journal of Nanomaterials
Volume 2012, Article ID 345086, 6 pages
doi:10.1155/2012/345086

Research Article

Align Ag Nanorods via Oxidation Reduction Growth Using RF-Sputtering

Zhan-Shuo Hu,[1] Fei-Yi Hung,[2] Shoou-Jinn Chang,[1] Wei-Kang Hsieh,[1] and Kuan-Jen Chen[3]

[1] *Institute of Microelectronics, Center for Micro/Nano Science and Technology, National Cheng Kung University, Tainan 701, Taiwan*
[2] *Department of Materials Science and Engineering, Center for Micro/Nano Science and Engineering, National Cheng Kung University, Tainan 701, Taiwan*
[3] *The Instrument Center, Institute of Nanotechnology and Microsystems Engineering, National Cheng Kung University, Tainan 701, Taiwan*

Correspondence should be addressed to Fei-Yi Hung, fyhung@mail.ncku.edu.tw

Received 2 March 2012; Revised 23 April 2012; Accepted 23 April 2012

Academic Editor: Amir Kajbafvala

Silver nanorod arrays grew on the individual metallic silver particles after the thermal decomposition of the silver oxides. The formation of silver oxide came from the input of oxygen during sputtering. The subsequent growth of the Ag nanorods started from the single silver grain that originated from the decomposition caused by thermal reduction. This method for oxidation reduction growth used no catalysts and improved the interface effect for the lattice match. Photoluminescence of Ag nanorods was detected at 2.17 eV.

1. Introduction

One-dimensional (1D) metal nanostructures, including rods, wires, and tubes, have recently attracted interest and been applied to optical-electronic and sensing nanodevices due to their unique optical and conductive properties and thermal conductivity [1–5]. Among the various metals, silver exhibits effective thermal conductivity and the highest electrical conductivity and can be synthesized into Ag-based compounds with different compositions. Silver is more reactive than gold or platinum; therefore, silver is the most favorable candidate for various applications [6, 7]. For the silver oxide system (Ag_xO), silver can be reduced by a thermal decomposition reaction due to its low melting point and active energy [8].

One-dimensional (1D) silver nanostructures are used as the substrates to detect surface enhanced Raman scattering (SERS) and surface plasmon resonance (SPR) and for enhancing the photoluminescence of the ZnO system [9–14]. Over the last decade, many methods have been used to fabricate Ag nanowires and nanorods. Xu et al. used porous alumina templates to carry out chemical deposition for the fabrication of silver nanorod arrays [15]. Chen et al. fabricated Ag nanowires via a polybasic process [16]. Murphy and Jana demonstrated a seed-mediated method for obtaining Ag nanowires [17]. All the aforementioned methods require a chemical solution or template to fabricate the Ag 1D nanostructure. To obviate the chemical solutions and reduce complexity, Zhao et al. grew Ag nanorod arrays using oblique angle deposition [18]. Mohanty et al. used vapor-solid phase synthesis to produce Ag nanowires [19]. Besides the aforementioned fabrications, a few literatures have demonstrated the formation of the various nanostructures by sputtering [20–23], and oxide-assisted growth has been developed for one-dimensional nanostructures in previous studies [24–26]. Notably, oxidation reduction growth (ORG) of 1D metal structures prepared using a sputtering method has never been reported. Additionally, when the bulk metal reduces to nanoscale, the luminescence will affect the electron-hole recombination due to the larger aspect ratio [27, 28].

This study has demonstrated an oxidation reduction growth (ORG) technique with mixed-gas sputtering to create Ag nanorod arrays without any chemical solutions or contamination from aqueous solution via oxide-assisted growth [29]. The ORG methodology is used to deposit an Ag buffer layer with silver oxide nanoclusters to obtain Ag

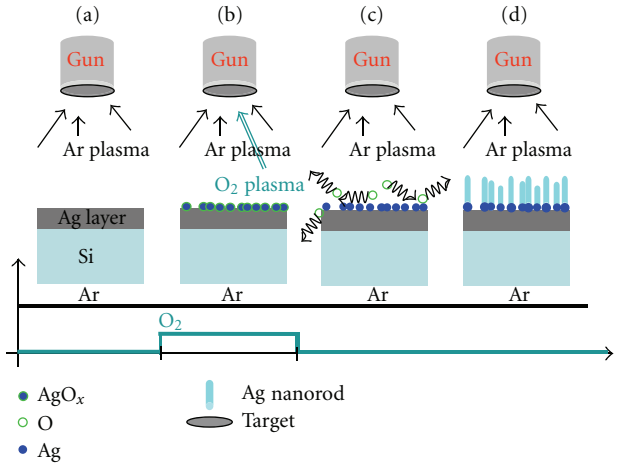

FIGURE 1: Growth mechanism of Ag nanorod arrays during sputtering process.

nanorods arrays using a two-step mixed gaseous process. The success of the technique provides support for the oxidation reduction growth (ORG) mechanism and proves suitable for fabrication of Ag nanorods in the semiconductor industry.

2. Experiment

Prior to sputtering, a p-Si (100) substrate was first cleaned in acetone and then cleaned in isopropanol for 300 s. The p-Si substrate was then dipped into hydrofluoric acid to remove the native oxide and finally rinsed with deionized water. For RF sputtering, the cleaned p-Si was loaded into the sputter chamber to perform sputtering, and the distance between the sample surface and silver target was approximately 3 cm.

The RF sputter system was evacuated to below 1.8×10^{-4} Torr, and argon gas was introduced with the flow rate controlled at 15 sccm. The gas pressure was fixed at 15×10^{-3} Torr during the sputtering process, and the RF power was set at 80 W. The sputtering times are 20 and 30 min for silver oxide clusters and silver nanorods, respectively. The deposition rates of silver, silver oxide, and nanorods are 3, 1, and 10 nm/min, respectively. The amount of the introduced oxygen is 1 sccm during reactive sputtering.

A schematic diagram for the oxidation reduction growth of silver nanorods is illustrated in Figure 1. The whole sputtering process was continuous without venting until Ag nanorods had grown. In Figure 1(a), at the beginning of sputtering, a thin silver film was predeposited on the Si surface with a constant flow of 15 sccm argon gas. Next, a trace of oxygen was introduced and mixed with argon as the source of plasma to form the silver oxide seed during sputtering, as shown in Figure 1(b). The silver oxide seed randomly dispersed over the Ag buffer layer and was able to form the contiguous thin film due to the trace amounts of oxygen. Notably, the melting point of silver oxide is normally approximately 300°C and even lower at the nanoscale [8]. When engaged in the sputtering process, the temperature of the sample will rise to between 200°C and 300°C allowing silver oxide to dissolve and release O_2 and return the silver to the original silver oxide site (Figure 1(c)). In Figure 1(d), sputtering is performed without oxygen, and the silver nanorods start to grow from the reduction metal silver site. The oxidation reduction growth (ORG) of silver nanorods is a novel and continual process, which uses sputtering.

The morphology of the Ag nanorods was investigated by scanning electron microscopy (SEM), and the crystallization of the silver nanorods and silver oxide seeds were examined using X-ray diffraction (XRD). The incident angle of X-ray was fixed 1° for the phase identification of the extreme surface. For the detailed structure, the orientation was detected by transmission electron microscopy (TEM), and the selected area electron diffraction (SAED) was observed on the body of the nanorods and the silver buffer layer. For PL measurements, a 405 nm laser was used as an excitation light, and detection was performed in a photomultiplier tube.

3. Results and Discussions

Figure 2 shows tilted view SEM images and glancing angle XRD for the silver oxide seeds under sputtering 20 min and Ag nanorods under sputtering 30 min. As shown in Figures 2(a) and 2(b), not only were the silver oxide seeds observed but also the Ag nanorods uniformly distributed over the sample surface. Notably, the density of the silver oxide seeds was approximately 150/um^2, approaching that of Ag nanorods. The range for the diameters of the Ag nanorods was from 40 to 55 nm while the diameter of the silver oxide seeds was approximately 60 nm. The average diameter of the Ag nanorods was slightly smaller than that of the silver oxide seeds.

The energy dispersive spectrometer (EDS) data of the Ag nanorods is exhibited in Figure 2(c). A main peak of silver and a weak oxygen signal can be observed on the spectrum. According to the ratio of weight between Ag and oxygen, most of the peaks were Ag, and these were initially identified as pure Ag nanorods. The inset of Figure 2(c) is a cross section view of the Ag nanorods using a focused ion beam and most of the Ag nanorods aligned to the substrate. A silver buffer layer existed beneath the Ag nanorods, and this result is consistent with previous reports (not the present growth method) that one-dimensional aligned nanostructures also require the same material layer to grow due to the lattice match [30–33]. The thickness of the present Ag buffer layer was about 45 nm, and the length of the Ag nanorods was from 250 to 300 nm.

The crystallization of both the silver oxide nanoseeds and Ag nanorods was investigated using glancing angle XRD. Figure 2(d) shows the main Ag peaks, including (111), (200), (220), and (311), which coincide with the thin silver film [34]. In Ag nanorods case, all signals really came from Ag nanorods due to glancing angle XRD with 1° incidence, but the peaks of Ag signal in silver oxide nanoseeds resulted from the Ag buffer layer. Notably, the signal of silver oxide $(11\bar{1})$ appears at 28° in some of the silver oxide nanoclusters in addition to the Ag peaks. The silver oxide phase was Ag_3O_4 and was produced during the mixed-gas sputtering process with the input of oxygen [35, 36]. After the thermal

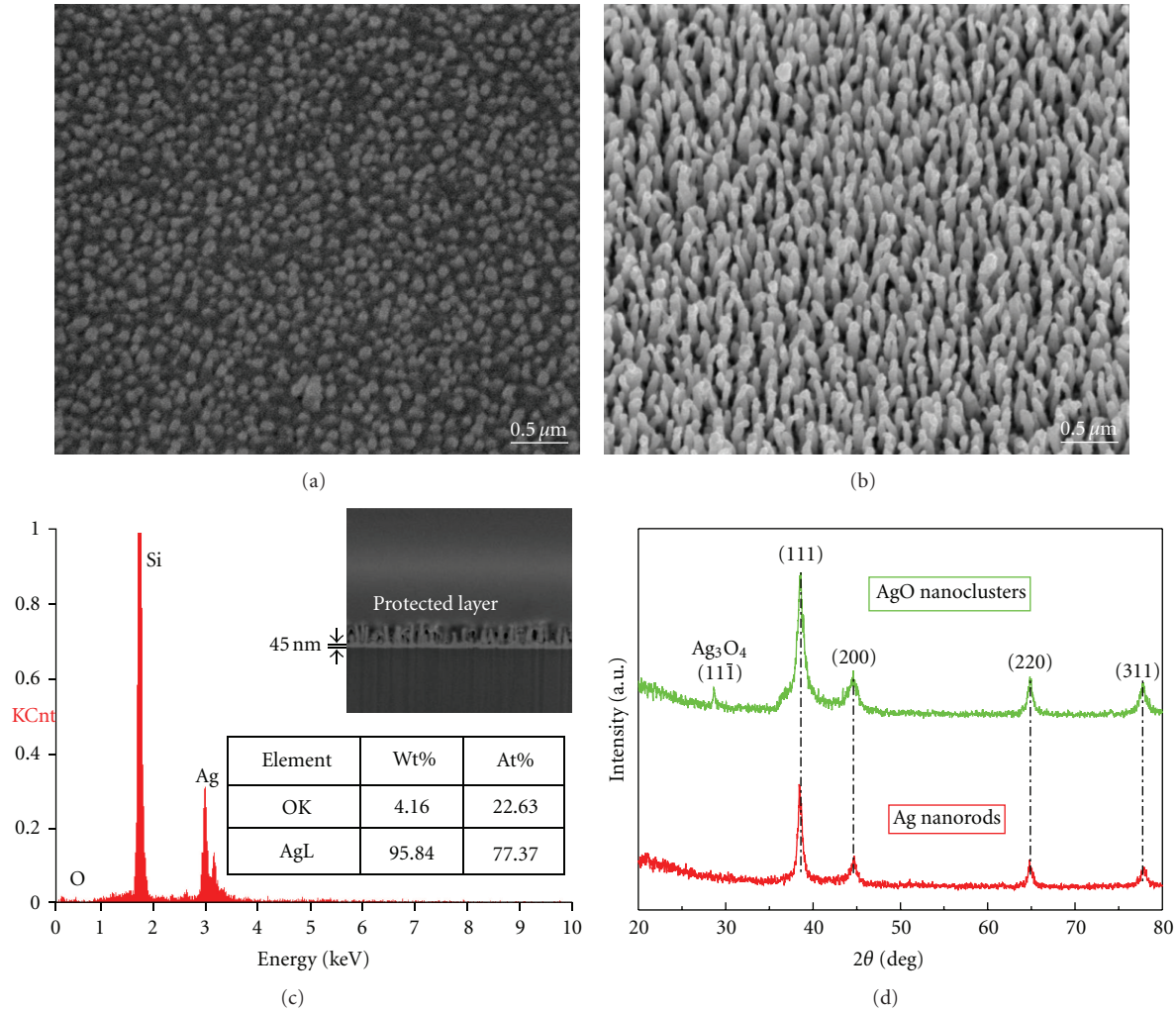

Figure 2: SEM images of (a) silver oxide nuclei, (b) Ag nanorod arrays, (c) EDS of Ag nanorods. The inset SEM image is a cross-section of Ag nanorods. (d) XRD spectra of Ag nanorods and silver oxide clusters.

decomposition, the oxygen resulting from the reduction reaction of silver oxides was pumped out. In addition, the production of silver oxides reduced metallic silver seeds for the growth of Ag nanorods. However, when the Ag_3O_4 phase is compared with the AgO phase, the Ag_3O_4 phase is more thermodynamically unstable (lower free energy) [37, 38]; therefore, the Ag_3O_4 can easily react in the consequent sputtering process to induce the growth of Ag nanorods with a chemical reaction of $Ag_3O_{4(s)} \rightarrow 3Ag_{(s)} + 2O_{2(g)}$ [39]. This two-step oxidation reduction process is responsible for the growth of the nanorods. Therefore, the present oxidation reduction growth (ORG) mechanism can also be applied to other metal systems with low melting point [40].

Figure 3(a) shows TEM observations with Ag nanorods aligned to the Ag buffer layer, and the corresponding SAED pattern from the white circle zone is shown in Figure 3(b). According to the electron diffraction pattern, the Ag nanorods were ascertained to be the single-crystal structure; the high resolution TEM image is shown in Figure 3(c). Additionally, the Ag nanorods grow from the thermal-reduced Ag nucleus above the Ag buffer layer. A lattice image of the interfacial layer between the Ag nanorods and the grain is shown in the Figure 3(d), which demonstrates a perfect lattice arrangement. Figure 3(b) also shows that the Ag nanorods are crystalline and the interface zones between the Ag nanorods and the thermal-reduced Ag nucleus are coherent. From the cross-section observation, the Ag buffer layer was composed of many silver grains and this result was coincident with the phases of XRD spectra (Figure 2(d)). Notably, the Ag nanorods of the ORG structure also possessed excellent properties.

A PL spectrum of the Ag nanorod arrays under the irradiation of a 408 nm laser could be seen in Figure 4. The spectra ranges of all samples, which exhibit the strongest intensity near 2.17 eV, were from ~1.9 to ~2.45 eV. Basically, PL peaks in the visible wavelength can be regarded as a radiative recombination between Fermi level electrons and *sp*- or *d*-band holes [39, 41]. However, silver oxide forms easily in air and it may also provide a possible route of luminescence for photoreduced metallic Ag under visible

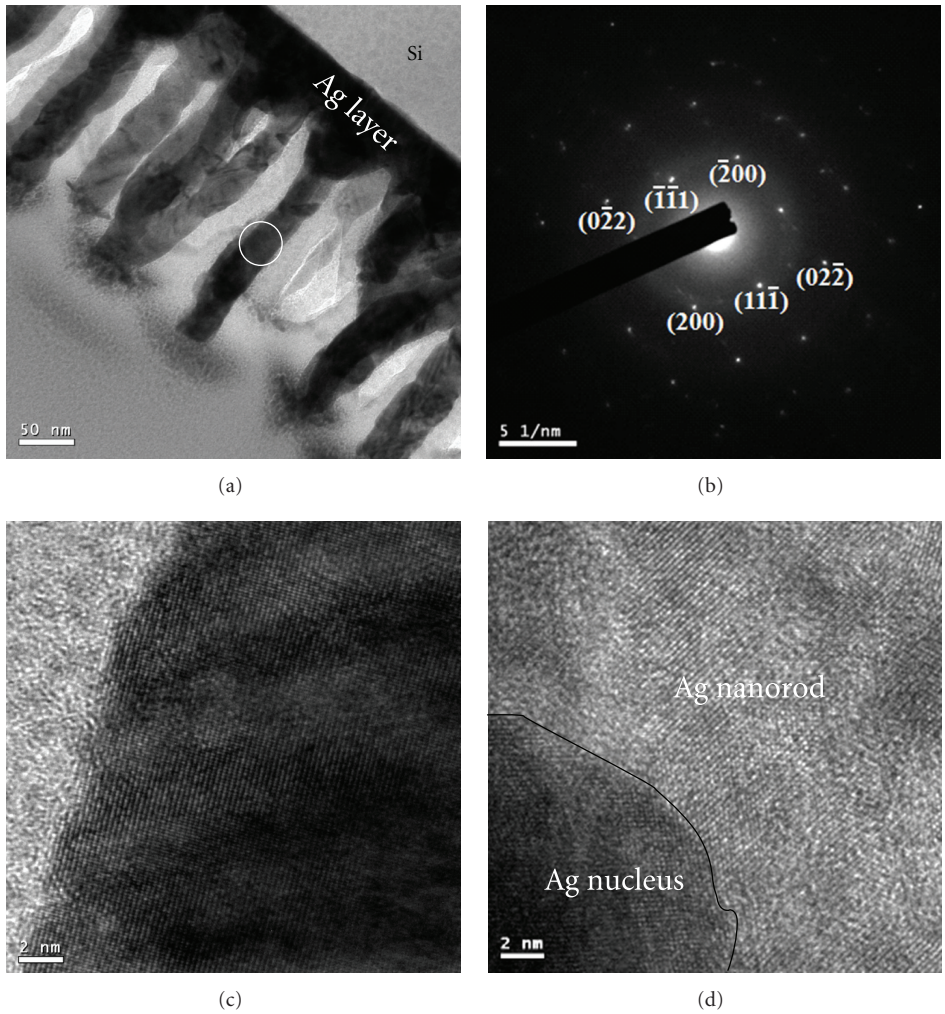

Figure 3: (a) A typical TEM image of Ag nanorods. (b) SAED of the white circle in (a), (c) the HRTEM image of Ag nanorod, (d) the interface between Ag nanorod and reduced metal nucleus.

illumination [27, 42]. Herein, PL spectrum of Ag nanorods was also measured under the vacuum to avoid the formation of silver oxide during the irradiation of laser in air, and there is no shift for the spectra of Ag nanorods both in air and in vacuum.

4. Conclusion

In summary, Ag nanorods were fabricated using an oxidation reduction growth (ORG) method by sputtering without catalysts or chemical solutions. The Ag nanorods grew in the original locations of reduced metal nuclei after thermal composition of silver oxide nanoclusters. The Ag nanorods stood vertically on the Ag buffer interlayer and grew from the interface between the Ag grains and the Ag buffer interlayer. PL spectra of Ag nanorods both in air and vacuum were observed at 2.17 eV due to the photoactivation caused by a radiative recombination of Fermi level electrons and d-band holes.

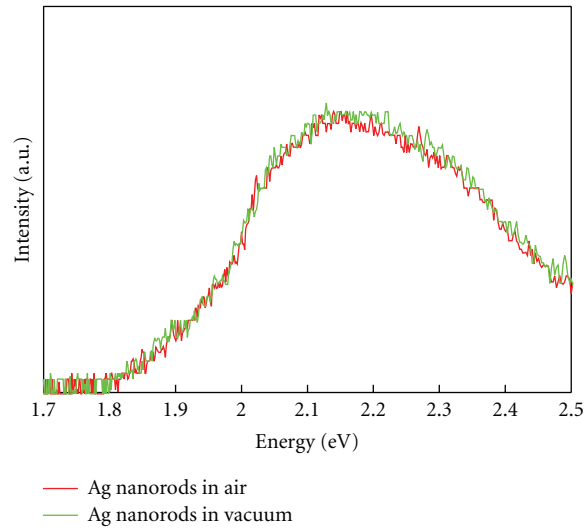

Figure 4: Room temperature PL spectra of Ag nanorods and silver oxide clusters.

Acknowledgments

The authors are grateful to The Instrument Center of National Cheng Kung University, the Center for Micro/Nano Science and Technology (D101-2700) and NSC 100-2221-E-006-093; NSC 100-2221-E-006-094; NSC 100-2622-E-006-030-CC for the financial support.

References

[1] J. I. Pascual, J. Méndez, J. Gómez-Herrero et al., "Properties of metallic nanowires: from conductance quantization to localization," *Science*, vol. 267, no. 5205, pp. 1793–1795, 1995.

[2] M. C. Daniel and D. Astruc, "Gold Nanoparticles: assembly, supramolecular chemistry, quantum-size-related properties, and applications toward biology, catalysis, and nanotechnology," *Chemical Reviews*, vol. 104, no. 1, pp. 293–346, 2004.

[3] A. R. Tao and P. Yang, "Polarized surface-enhanced Raman spectroscopy on coupled metallic nanowires," *Journal of Physical Chemistry B*, vol. 109, no. 33, pp. 15687–15690, 2005.

[4] I. R. Gould, J. R. Lenhard, A. A. Muenter, S. A. Godleski, and S. Farid, "Two-electron sensitization: a new concept for silver halide photography," *Journal of the American Chemical Society*, vol. 122, no. 48, pp. 11934–11943, 2000.

[5] B. J. Murray, E. C. Walter, and R. M. Penner, "Amine vapor sensing with silver mesowires," *Nano Letters*, vol. 4, no. 4, pp. 665–670, 2004.

[6] Y. Sun, "Conversion of Ag nanowires to AgCl nanowires decorated with Au nanoparticles and their photocatalytic activity," *Journal of Physical Chemistry C*, vol. 114, no. 5, pp. 2127–2133, 2010.

[7] U. Lee, S. Ham, C. Han, Y. J. Jeon, N. Myung, and K. Rajeshwar, "Mild and facile synthesis of Ag_2S nanowire precursor using mercaptoacetic acid as a reductant/stabilizer and its subsequent conversion to Ag_2S or CdS nanowires," *Materials Chemistry and Physics*, vol. 121, no. 3, pp. 549–554, 2010.

[8] G. I. N. Waterhouse, G. A. Bowmaker, and J. B. Metson, "The thermal decomposition of silver (I, III) oxide: a combined XRD, FT-IR and Raman spectroscopic study," *Physical Chemistry Chemical Physics*, vol. 3, no. 17, pp. 3838–3845, 2001.

[9] Q. Zhou, Y. Yang, J. Ni, Z. Li, and Z. Zhang, "Rapid recognition of isomers of monochlorobiphenyls at trace levels by surface-enhanced Raman scattering using Ag nanorods as a substrate," *Nano Research*, vol. 3, no. 6, pp. 423–428, 2010.

[10] P. H. C. Camargo, C. M. Cobley, M. Rycenga, and Y. Xia, "Measuring the surface-enhanced Raman scattering enhancement factors of hot spots formed between an individual Ag nanowire and a single Ag nanocube," *Nanotechnology*, vol. 20, no. 43, Article ID 434020, 2009.

[11] Y. J. Liu, Z. Y. Zhang, Q. Zhao, R. A. Dluhy, and Y. P. Zhao, "Surface enhanced Raman scattering from an ag nanorod array substrate: the site dependent enhancement and layer absorbance effect," *Journal of Physical Chemistry C*, vol. 113, no. 22, pp. 9664–9669, 2009.

[12] W. Wei, L. Shuzhou, Q. Lidong et al., "Surface Plasmon-Mediated energy transfer in heterogap Au-Ag nanowires," *Nano Letters*, vol. 8, no. 10, pp. 3446–3449, 2008.

[13] J. Zhu, "Surface plasmon resonance from bimetallic interface in Au-Ag core-shell structure nanowires," *Nanoscale Research Letters*, vol. 4, no. 9, pp. 977–981, 2009.

[14] P. Cheng, D. Li, X. Li, T. Liu, and D. Yang, "Localized surface plasmon enhanced photoluminescence from ZnO films: extraction direction and emitting layer thickness," *Journal of Applied Physics*, vol. 106, no. 6, Article ID 063120, 2009.

[15] J. Xu, G. A. Cheng, and R. T. Zheng, "Controllable synthesis of highly ordered Ag nanorod arrays by chemical deposition method," *Applied Surface Science*, vol. 256, no. 16, pp. 5006–5010, 2010.

[16] C. Chen, L. Wang, G. Jiang et al., "The influence of seeding conditions and shielding gas atmosphere on the synthesis of silver nanowires through the polyol process," *Nanotechnology*, vol. 17, no. 2, pp. 466–474, 2006.

[17] C. J. Murphy and N. R. Jana, "Controlling the aspect ratio of inorganic nanorods and nanowires," *Advanced Materials*, vol. 14, no. 1, pp. 80–82, 2002.

[18] Y. P. Zhao, S. B. Chaney, and Z. Y. Zhang, "Absorbance spectra of aligned Ag nanorod arrays prepared by oblique angle deposition," *Journal of Applied Physics*, vol. 100, no. 6, Article ID 063527, 2006.

[19] P. Mohanty, I. Yoon, T. Kang et al., "Simple vapor-phase synthesis of single-crystalline Ag nanowires and single-nanowire surface-enhanced raman scattering," *Journal of the American Chemical Society*, vol. 129, no. 31, pp. 9576–9577, 2007.

[20] U. Schürmann, W. Hartung, H. Takele, V. Zaporojtchenko, and F. Faupel, "Controlled syntheses of Ag-polytetrafluoroethylene nanocomposite thin films by co-sputtering from two magnetron sources," *Nanotechnology*, vol. 16, no. 8, pp. 1078–1082, 2005.

[21] D. K. Avasthi, Y. K. Mishra, D. Kabiraj, N. P. Lalla, and J. C. Pivin, "Synthesis of metal-polymer nanocomposite for optical applications," *Nanotechnology*, vol. 18, no. 12, Article ID 125604, 2007.

[22] Y. T. Lin, C. Y. Chen, C. P. Hsiung, K. W. Cheng, and J. Y. Gan, "Growth of RuO_2 nanorods in reactive sputtering," *Applied Physics Letters*, vol. 89, no. 6, Article ID 063123, 2006.

[23] K. W. Cheng, Y. T. Lin, C. Y. Chen et al., "*In situ* epitaxial growth of TiO_2 on RuO_2 nanorods with reactive sputtering," *Applied Physics Letters*, vol. 88, no. 4, Article ID 043115, pp. 1–3, 2006.

[24] X. M. Meng, J. Q. Hu, Y. Jiang, C. S. Lee, and S. T. Lee, "Oxide-assisted growth and characterization of Ge/SiOx nanocables," *Applied Physics Letters*, vol. 83, no. 11, pp. 2241–2243, 2003.

[25] R. Q. Zhang, Y. Lifshitz, and S. T. Lee, "Oxide-assisted growth of semiconducting nanowires," *Advanced Materials*, vol. 15, no. 7-8, pp. 635–640, 2003.

[26] C. L. Pint, S. T. Pheasant, A. N. G. Parra-Vasquez, C. Horton, Y. Xu, and R. H. Hauge, "Investigation of optimal parameters for oxide-assisted growth of vertically aligned single-walled carbon nanotubes," *Journal of Physical Chemistry C*, vol. 113, no. 10, pp. 4125–4133, 2009.

[27] L. A. Peyser, A. E. Vinson, A. P. Bartko, and R. M. Dickson, "Photoactivated fluorescence from individual silver nanoclusters," *Science*, vol. 291, no. 5501, pp. 103–106, 2001.

[28] M. Nirmal and L. Brus, "Luminescence photophysics in semiconductor nanocrystals," *Accounts of Chemical Research*, vol. 32, no. 5, pp. 407–414, 1999.

[29] A. Borras, M. MacIas-Montero, P. Romero-Gomez, and A. R. Gonzalez-Elipe, "Supported plasma-made 1D heterostructures: perspectives and applications," *Journal of Physics D*, vol. 44, no. 17, Article ID 174016, 2011.

[30] H. Jung, R. Kuljic, M. A. Stroscio, and M. Dutta, "Confinement in PbSe wires grown by rf magnetron sputtering," *Applied Physics Letters*, vol. 96, no. 15, Article ID 153106, 2010.

[31] S. W. Kang, S. K. Mohanta, Y. Y. Kim, and H. K. Cho, "Realization of vertically well-aligned ZnO:Ga nanorods by magnetron

sputtering and their field emission behavior," *Crystal Growth and Design*, vol. 8, no. 5, pp. 1458–1460, 2008.

[32] C. Li, G. Fang, L. Yuan et al., "Field emission from carbon nanotube bundle arrays grown on self-aligned ZnO nanorods," *Nanotechnology*, vol. 18, no. 15, Article ID 155702, 2007.

[33] M. Suzuki, K. Nagai, S. Kinoshita et al., "Vapor phase growth of AI whiskers induced by glancing angle deposition at high temperature," *Applied Physics Letters*, vol. 89, no. 13, Article ID 133103, 2006.

[34] S. Iida, T. Okui, T. Tai, and S. Akao, "Thin Ag film formation onto Si/SiO_2 substrate," *Applied Surface Science*, vol. 166, no. 1, pp. 160–164, 2000.

[35] Z. S. Hu, F. Y. Hung, S. J. Chang et al., "Effects of Ag nanoshape and AgGa phase in Ag-Si nanostructure using 2-step etching process," *Journal of Alloys and Compounds*, vol. 509, no. 3, pp. 758–763, 2011.

[36] Z.-S. Hu, F.-Y. Hung, S.-J. Chang, K.-J. Chen, and Y.-Z. Chen, "Crystallization effect of Al-Ag alloying layer in PL enhancement of ZnO thin film," *Intermetallics*, vol. 18, no. 8, pp. 1428–1431, 2010.

[37] R. O. Suzuki, T. Ogawa, and K. Ono, "Use of ozone to prepare silver oxides," *Journal of the American Ceramic Society*, vol. 82, no. 8, pp. 2033–2038, 1999.

[38] T. Rosenqvist, *Principles of Extractive Metallurgy*, McGraw-Hill, New York, NY, USA, 1974.

[39] G. I. N. Waterhouse, J. B. Metson, and G. A. Bowmaker, "Synthesis, vibrational spectra and thermal stability of Ag_3O_4 and related Ag_7O_8X salts ($X = NO_3^-$, ClO_4^-, HSO_4^-)," *Polyhedron*, vol. 26, no. 13, pp. 3310–3322, 2007.

[40] V. I. Yukhvid, S. V. Maklakov, P. V. Zhirkov, V. A. Gorshkov, N. I. Timokhin, and A. Y. Dovzhenko, "Combustion synthesis and structure formation in a model $Cr\text{-}CrO_3$ self-propagating high-temperature synthesis system," *Journal of Materials Science*, vol. 32, no. 7, pp. 1915–1924, 1997.

[41] R. Sarkar, P. Kumbhakar, A. K. Mitra, and R. A. Ganeev, "Synthesis and photoluminescence properties of silver nanowires," *Current Applied Physics*, vol. 10, no. 3, pp. 853–857, 2010.

[42] C. Bürgel, R. Mitrić, and V. Bonacic-Koutecky, "Emissive properties of silver particles at silver oxide surface defects," *Applied Physics A*, vol. 82, no. 1, pp. 117–123, 2006.